

LOCAL PHENOMENA DURING RIVETING PROCESS

Jerzy Kaniowski
Wojciech Wronicz

Institute of Aviation, Warsaw, Poland

Abstract

The paper presents experimental and numerical study of the local phenomena during the riveting process.

It is commonly accepted that technological factors of the riveting process has a strong influence on the fatigue life of riveted joints. The authors analysed the papers concerned the experimental researches of the riveting force influence on fatigue life. The magnitude of the life increase caused by the riveting force increase suggests the authors that this is not only the result of beneficial stress system but the change of the joint formation mechanism has taken place. This was an inspiration to undertake more detailed researches of the riveting process.

The strain progress during the riveting process has been experimentally investigated for four types of aluminium rivets used in airframes. Measurements confirm very high strains near the driven head. For some types of rivets the reversal strain signal has been recorded. Several FE model has been use to investigate the riveting process. The axisymmetric and solid models were used. The agreement of experimental and numerical results in some cases were good, in other cases the numerical models demand further development. In any calculations, the reversal strain effect has not been obtained, This suggest that it is result of the phenomenon which has not been taken into account in numerical modelling.

The working hypothesis has been assumed that during the riveting process adhesive joints (called cold welding) were formed and destroyed during the process, what was the reason of the observed reversal strain signal. The authors are going to continue this investigation.

Keywords: Riveting, fatigue, strain gauge, FE, residual stress, airframes

INTRODUCTION

Although new materials such as composites and new joining techniques such as friction stir welding, have been successfully implemented into aerospace structures, riveting still remains the most popular and basic method of joining metal parts. This technique has been used since the very beginning of the aircraft history resulting in the accumulation of an enormous body of relevant knowledge and experience. But some phenomena related to riveted joints have not been explained yet and they are now subject of new research. Some published research findings have indicated that the fatigue life of riveted joints can be significantly increased [1], leading to extended aircraft service life and a decrease in operational costs.

The fatigue life of riveted joints directly depends on the existing stress state. This stress state is a result of residual stresses introduced in manufacturing (sheet rolling, riveting), modified by external loads to which a structure is exposed. Residual stresses induced by the riveting process represent a large proportion of total stresses since typically they exceed the yield point near the holes [2].

Some research has revealed that the stress state around the rivets depends on squeezing force and other factors such as a rivet type, material, clearance, etc. [2 - 5]. Other authors have demonstrated correlation between riveting force and fatigue life [1, 6]. Figure 1 presents tangential stresses around the rivet on the faying surface as a function of the radial position for the outer sheet (with a countersunk) (a), and the inner sheet (b), for several values of squeezing force. Figure 2 shows the fatigue life of three-row riveted joint for three levels of squeezing force permitted by the aircraft producer.

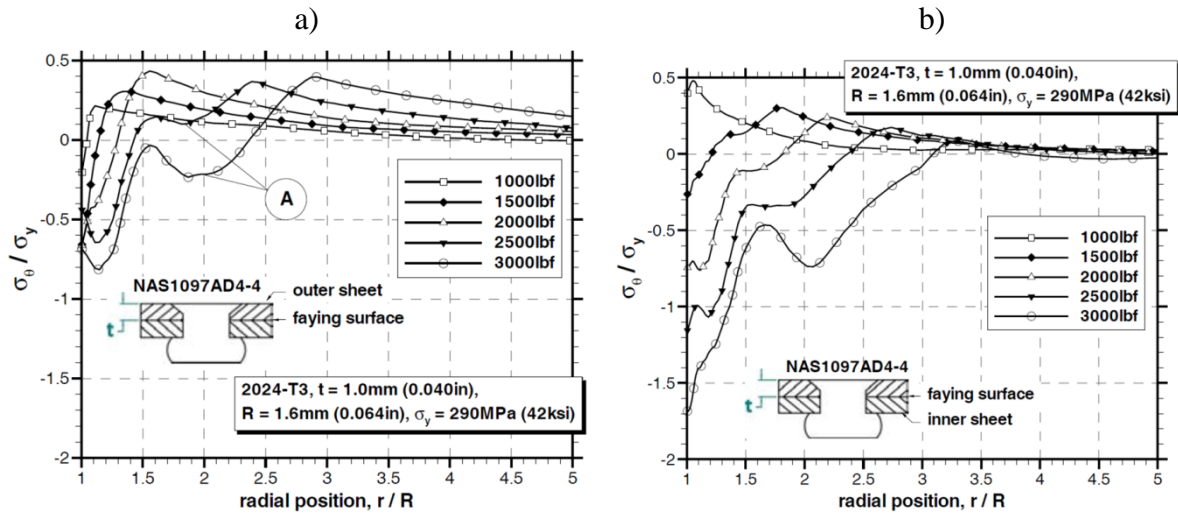


Fig. 1. Effect of the squeezing force value on the stress state around the rivet [3]

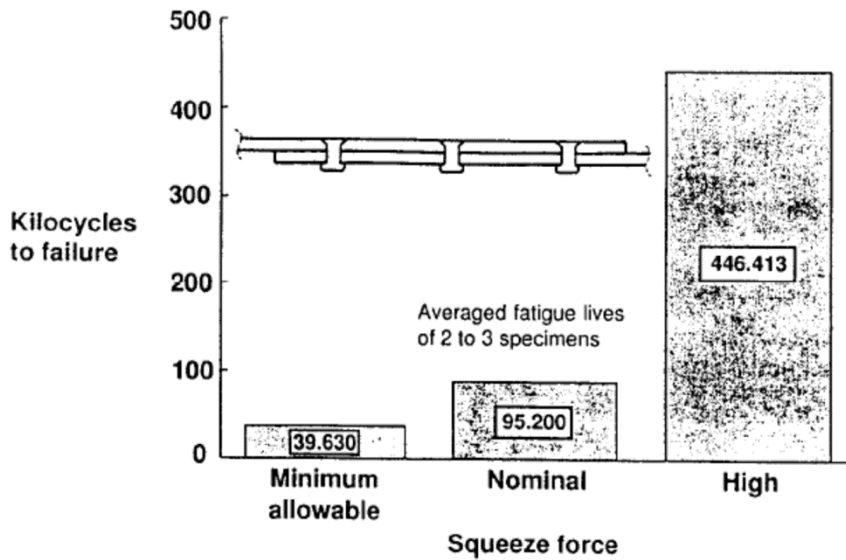


Fig. 2. Influence of the squeezing force value on the fatigue life of riveted joints [1]




More detailed results obtained by Müller and Hart-Smith [1] are presented in Table 1. Table 2 presents the configuration of specimens in these tests. The NACA riveting method consists of the installation of a rivet with a protruding head on the sheets with a countersunk (rivet head is on the side of the sheet without a countersunk). During riveting a driven head fills the countersunk and is then shaved (see rows 6-7 in Table 2).

Table 1. Selected results of fatigue tests of the three-row riveted joints published by Müller and Hart-Smith [1]

column ⇒ row ↓	1	2	3	4	5
1	Rivet type	Riveting force [kN]		D/D ₀	Cycles to failure [N]
2	Countersunk – 100°	Minimal	12	1,2	41 552 37 226 40 112
3		Nominal	17	1,4	97 535 99 624 88 442
4		High	36	1,7	451 270 441 556
5					Brazier
6	Brazier, NACA riveting method				983 764 1 035 000
7	Brazier, NACA riveting method, rivets in one row reversed				1 209 000 1 383 000 1 479 000

D/Do parameter: D-driven head diameter, Do-rivet shank diameter

Table 2. Configuration of specimens in the tests for which the results were presented in Table 1.

Row No. in Table 1	Configuration
2	
3	
4	
5	
6	
7	

The analysis of the Müller and Hart-Smith results [1] (Table 1) has revealed that when a 1.42-time increase in squeezing force (from 12 to 17 kN) resulted in a twofold increase in the fatigue life, then a three-time increase in squeezing force (from 12 to 36 kN, D/d parameter from 1.2 to 1.7) resulted in an eleven-time increase, while in the case of riveting with the NACA technology, even in a twenty-five and thirty-four-time increase in the fatigue life depending on a joint configuration. The magnitude of the life increase indicates that it is not only the result of the beneficial stress system but that a change in the joint formation mechanism has taken place.

STRAIN GAUGE MEASUREMENTS

The experiment with strain gauge measurements during the riveting process was designed and performed to investigate the strain state induced during the riveting process for several rivet types. The specimens used are presented in Figure 3.

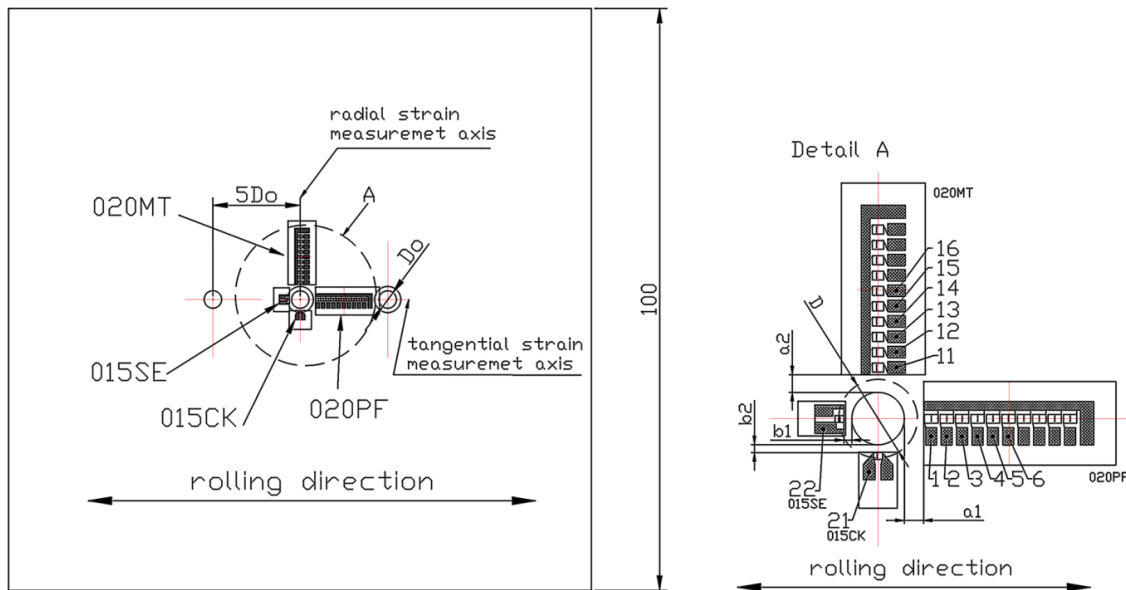


Fig. 3. Specimen geometry

The specimens consisted of two bare sheets made from 2024 T3 aluminium alloy with the nominal thickness of 1.27 mm and three rivets made from Polish aluminium alloy PA25/Russian alloy W65. First, the outer rivets were installed, afterwards the strain gauges were placed on the sheet surface near the driven head, and, finally, the central rivet was installed. Strain progress was recorded. Strip and micro gauges were used. The strip miniature gauges contained ten gauges (six were used), each with a length of 0.51 mm, located outside the driven head. The gauges worked during the whole riveting process. Besides those, two micro strain gauges with a length of 0.38 mm were placed very close to the rivet hole in the area, under the driven head after the riveting process. The gauges recorded strain until they were destroyed by the driven head. Riveting of the central rivet was carried out with a special riveting set to avoid damaging the gauges by the clamping sleeve used in the standard riveting set (Fig. 4). More detailed information about the experiment can be found in [4].

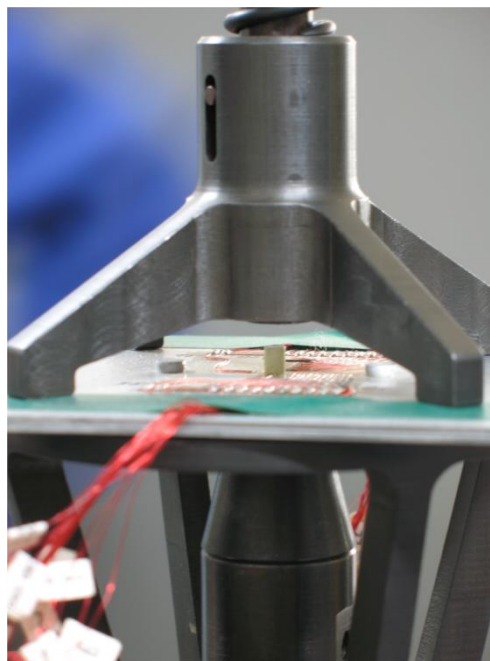


Fig. 4. Riveting with a special set

The experiment was performed for four types of rivets (Fig. 5):

- a) normal 90° countersunk rivet (according to the Polish aerospace standard BN-70/1121-04),
- b) 90° countersunk rivet with a compensator (according to the Russian aerospace standard ANU 301)
- c) normal brazier rivet (according to the Polish aerospace standard BN-70/1121-06)
- d) brazier rivet with a compensator (according to the Russian aerospace standard OST 1 34040 79).

Countersunk rivets had a diameter of 3 mm while brazier rivets had a diameter of 3.5 mm. In all specimens, central and outer rivets were of the same type and had the same dimensions.

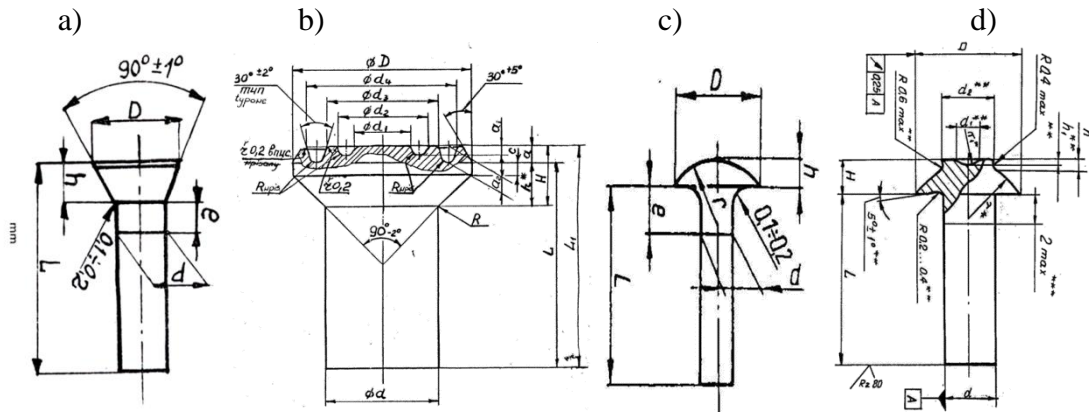
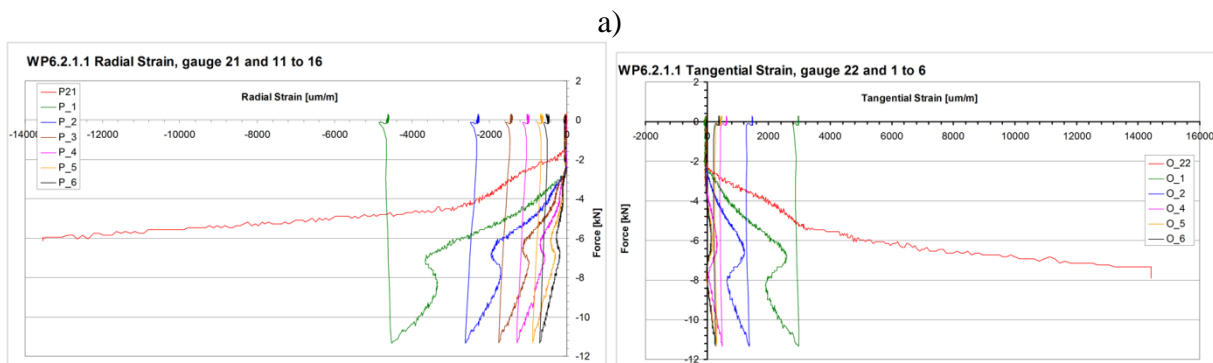


Fig. 5. Rivets used in the experiment

RESULTS OF MEASUREMENTS

The strain progress during the riveting process was illustrated in Figs. 6-9. The graphs present strains in the particular gauges as a function of squeezing force (gauge numbering according to Fig. 3: P21 denotes Gauge 21, P_1 to P_6 denote Gauges 11 to 16, O_22 denotes Gauge 22, O_1 to O6 denote Gauges 1 to 6). The highest values (of tension or compression) were obtained for gauges located closest to the hole. Figure 6 presents strains obtained for the normal countersunk rivet.



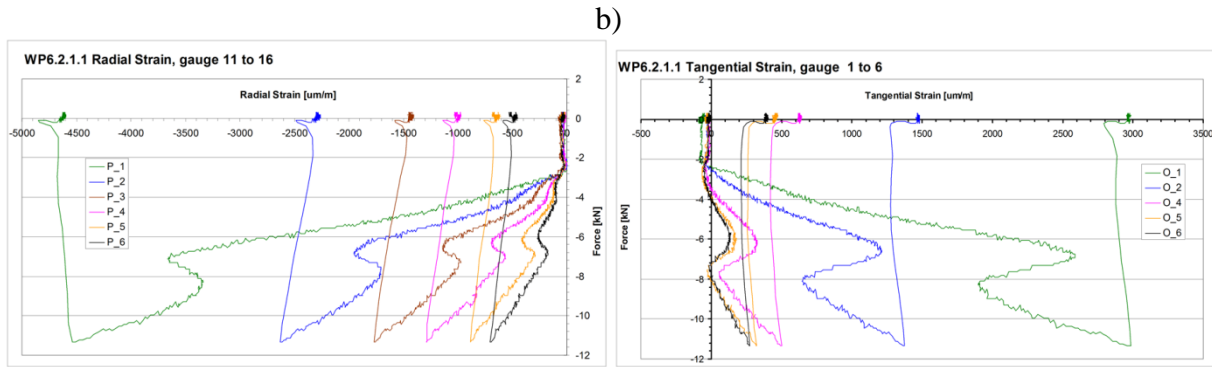


Fig. 6. Strains recorded during the riveting process for the normal countersunk rivet, a) all gauges, b) without micro-gauges

Microgauges located very close to the hole recorded very high strains. The reversal strain signal was recorded by all the gauges except micro-gauges, which were destroyed during the process. To better illustrate this phenomenon the results from micro-gauges were removed from the graph (Fig. 6b).

Figure 7 presents strains obtained for a countersunk rivet with a compensator.

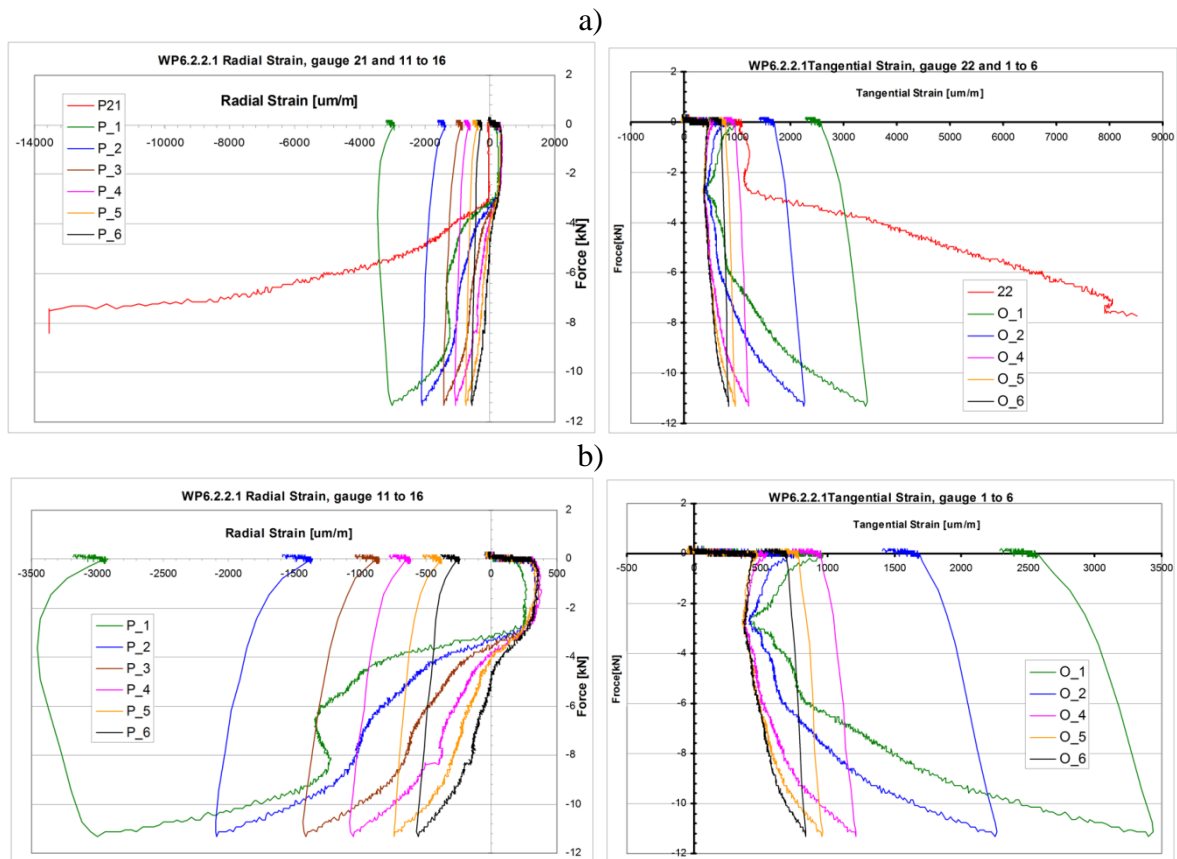


Fig. 7. Strains recorded during the riveting process for a countersunk rivet with a compensator, a) all gauges, b) without micro-gauges

Micro-gauges recorded radial strains of the same level as those obtained for the normal rivet, but tangential strains were significantly lower. In the case of radial strains, the reversal strain signal was recorded only by Gauge P_1 (section of the strip gauge closest to the rivet hole). In the case of tangential strains, the reversal signal could be observed for all the gauges at the beginning

of the riveting process. It was probably an effect of the specimens' bending. Elastic relaxation (springback) was definitely higher than in the case of the normal rivet.

Figure 8 presents strains obtained for the normal brazier rivet.

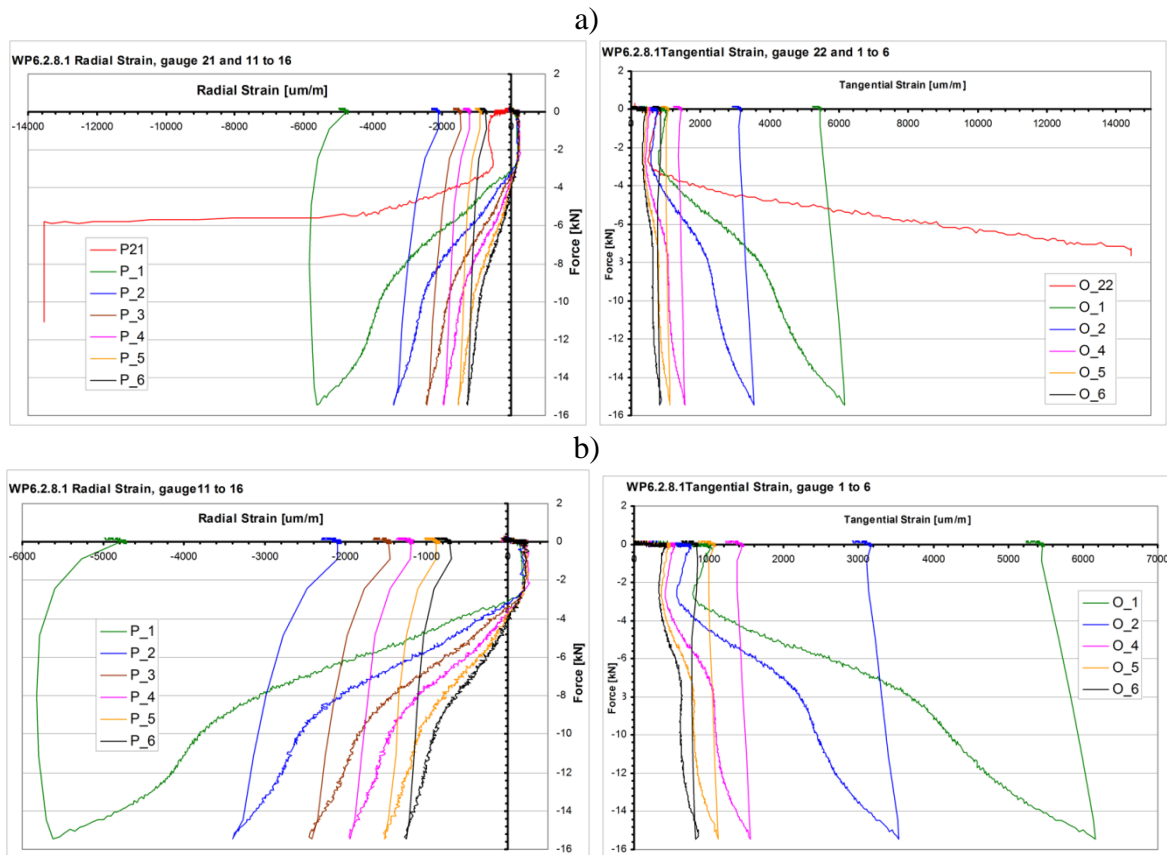


Fig. 8. Strains recorded during the riveting process for the normal brazier rivet, a) all gauges, b) without micro-gauges

Micro-gauges recorded strains at levels identical to those obtained for a normal countersunk rivet. The reversal strain signal was not visible for any gauges. The shape of curves in the relaxation phase (after maximum force) was similar to the results obtained for a countersunk rivet with a compensator.

Figure 9 presents strains obtained for a brazier rivet with a compensator.

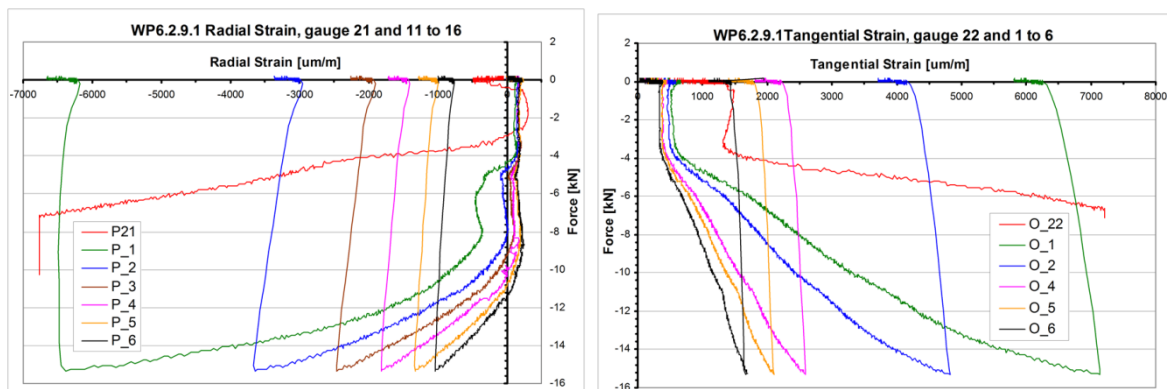


Fig. 9. Strains recorded during the riveting process for a brazier rivet with a compensator

The strains recorded by micro-gauges were about two times lower than those obtained for other types of investigated rivets. The reversal strain signal was recorded only by Gauge P_1 (radial strains, section of the strip gauge closest to the rivet hole). Elastic relaxation was similar to that observed in the case of a brazier rivet with a compensator.

The 'S' shaped strain progresses were recorded for countersunk rivets and the brazier rivet with a compensator. In the case of the normal countersunk rivet this effect was recorded by all strip gauges (radial and tangential strains); in other cases, only by isolated gauges measuring radial strains.

Similar shapes of strain plots can be found in [7] and [8]. Both papers analysed strain during the riveting process for countersunk rivets. Langrand et al. [7] explain the reversal strain signal as a result of the so called 'lug formation' at the hole edge, under the driven head. The analysis of the microsection of selected specimens riveted at the Institute of Aviation did not confirm the existence of such deformation (Fig. 10). The existence of a chamfer at the hole edge prevented its formation. In spite of that, the 'S'-shaped strain signals were recorded.

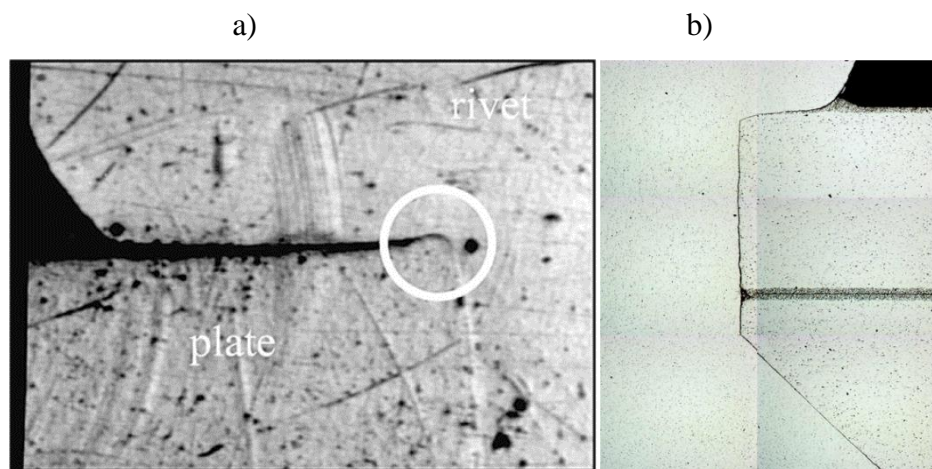


Fig. 10. Microsections of rivets after the riveting process, a) [7], b) own research

Li et al [8] explain this phenomenon by the presence of a clearance between the sheet and the rivet (distance of the rivet head above the sheet surface). Numerical calculations did not confirm this hypothesis. Moreover, this effect was also observed for a brazier rivet.

FEM CALCULATIONS

The experiment described above was analyzed with FEM. Nonlinear implicit algorithms were used to simulate the quasi-static riveting process (MSC MARC). Geometrical and material nonlinearity as well as contact phenomena were taken into account. Special boundary conditions resulting from the use of the special riveting set were modeled.

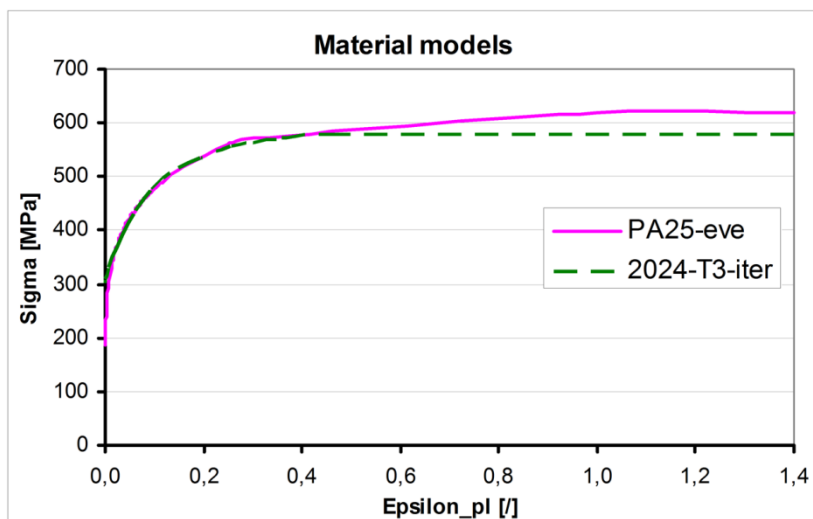


Fig. 11. Material models

Solid as well as axisymmetric elements were used. The brazier rivets (normal and with a compensator) were analyzed with the solid and axisymmetric modes, while in the case of the normal countersunk rivet only the axisymmetric model was used. More detailed information about calculations can be found in [4] and [9].

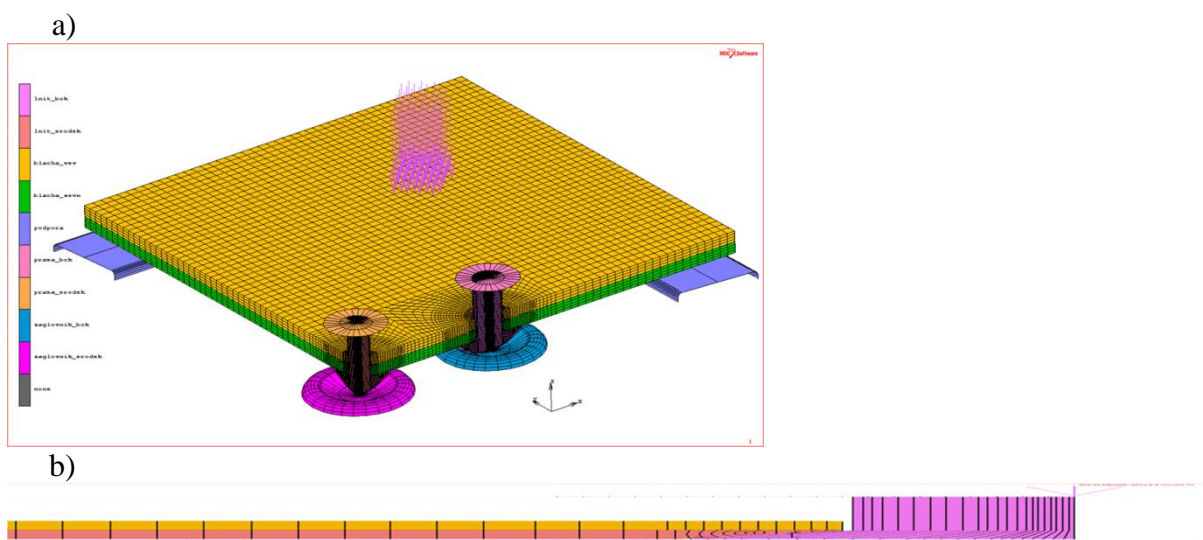


Fig. 12. Numerical models, a) solid, b) axisymmetric

The solid model consisted of four deformable contact bodies (two rivets and two sheets) and five rigid contact bodies (two holds-on, two press punches and the support of a special riveting set). Only a quarter of all specimens were modeled due to the symmetry. At first, the outer rivet was installed, then the central rivet. Correct results were not obtained for the brazier rivet with a compensator.

In the case of the axisymmetric model, there were three deformable contact bodies (rivet and two sheets, and three rigid contact bodies (a hold-on, a press punch and the support). Only the presence of the central rivet was taken into account (the outer rivets were neglected). Moreover, the model represented a circular specimen (axisymmetric analysis) with a diameter equal to the side length of real specimens. The results show that such simplification is acceptable and does not influence the results near the rivet in a significant way.

Figure 13 Illustrates some examples of stresses obtained for different models.

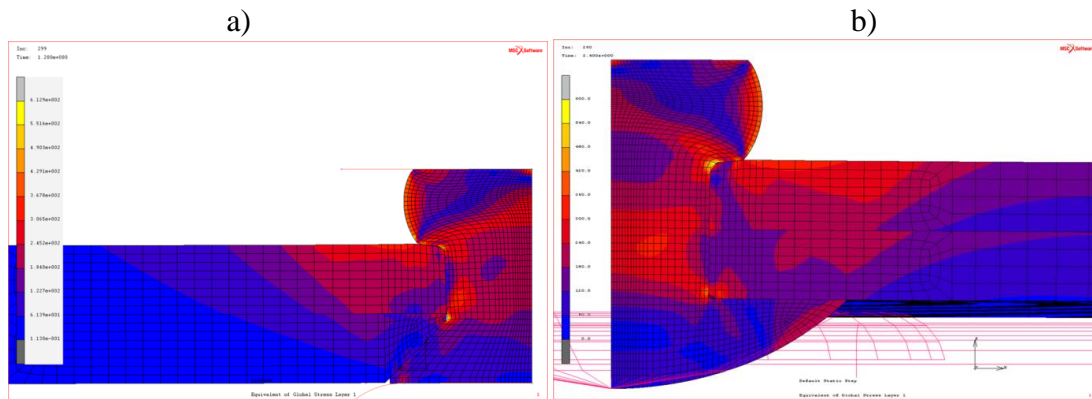


Fig. 13. Equivalent stresses (HMH) and deformation at the end of the riveting, a) normal countersunk rivet – the axisymmetric model, b) normal brazier rivet – the solid model

Strains measured in the experiment and strains obtained in numerical calculations are compared in Tables 3-5. In each table, the first row contains graphs of strains recorded by the section of the strip gauge closest to the rivet hole and for the two nodes of the FEM models that were placed closest to this gauge's centre. A series designation indicates the type of results (Gauge, Axi-FEM axisymmetric model, 3D-FEM solid model) and the distance between the node and the gauge centre. The graphs in the second row present strain distribution at the end of the riveting process (strain as a function of the distance from the rivet axis).

Table 3 presents the results for the normal countersunk rivet.

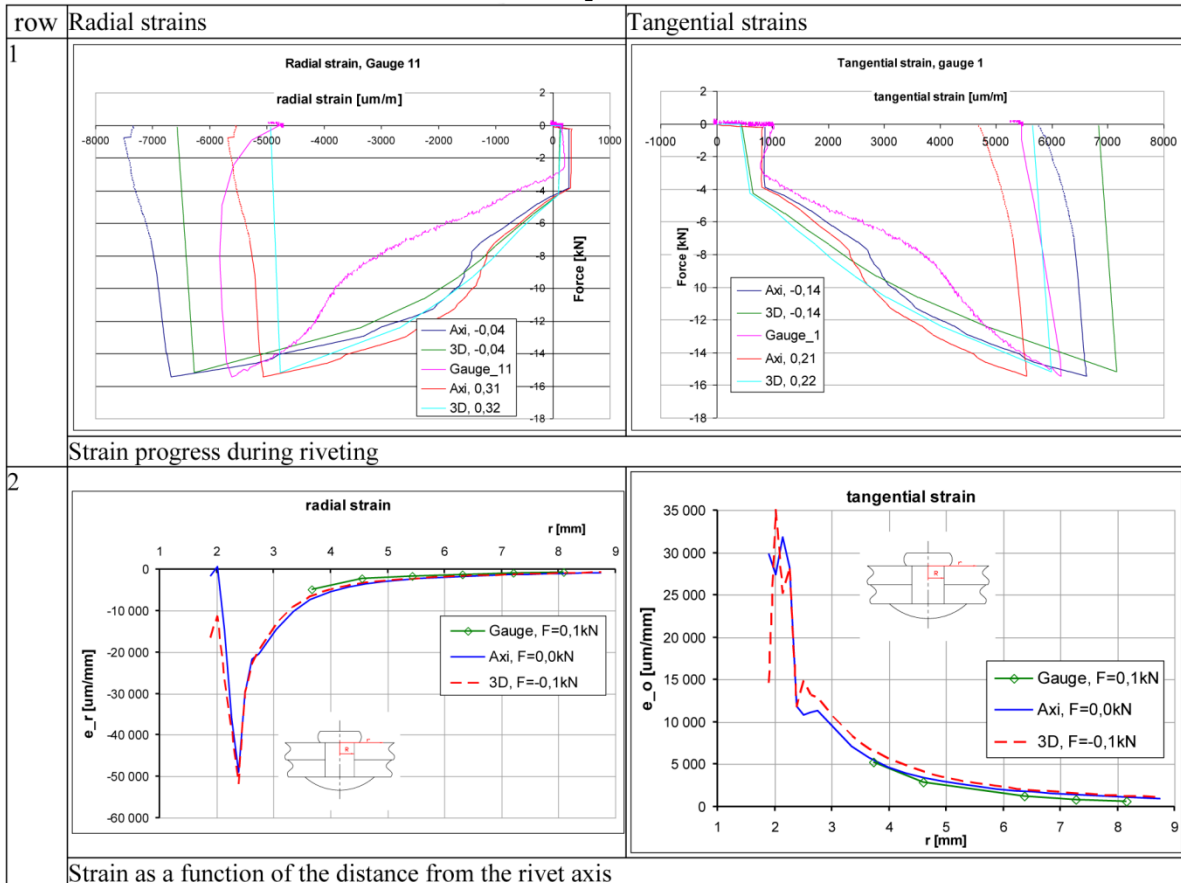
Table 3. Strains around the normal countersunk rivet - experiment and calculations

row	Radial strains	Tangential strains
1		
Strain progress during riveting		
2		
Strain as a function of the distance from the rivet axis		

In the case of radial strains, good correlation with the experiment at the end of the process is visible. In the case of tangential strains, numerical results are overestimated. During the riveting process, the numerical model does not agree with the experiment and the reversal strain signal has not been obtained in the calculations. The character of elastic relaxation is similar for the experimental and numerical results.

Table 4 presents the results for the normal brazier rivet.

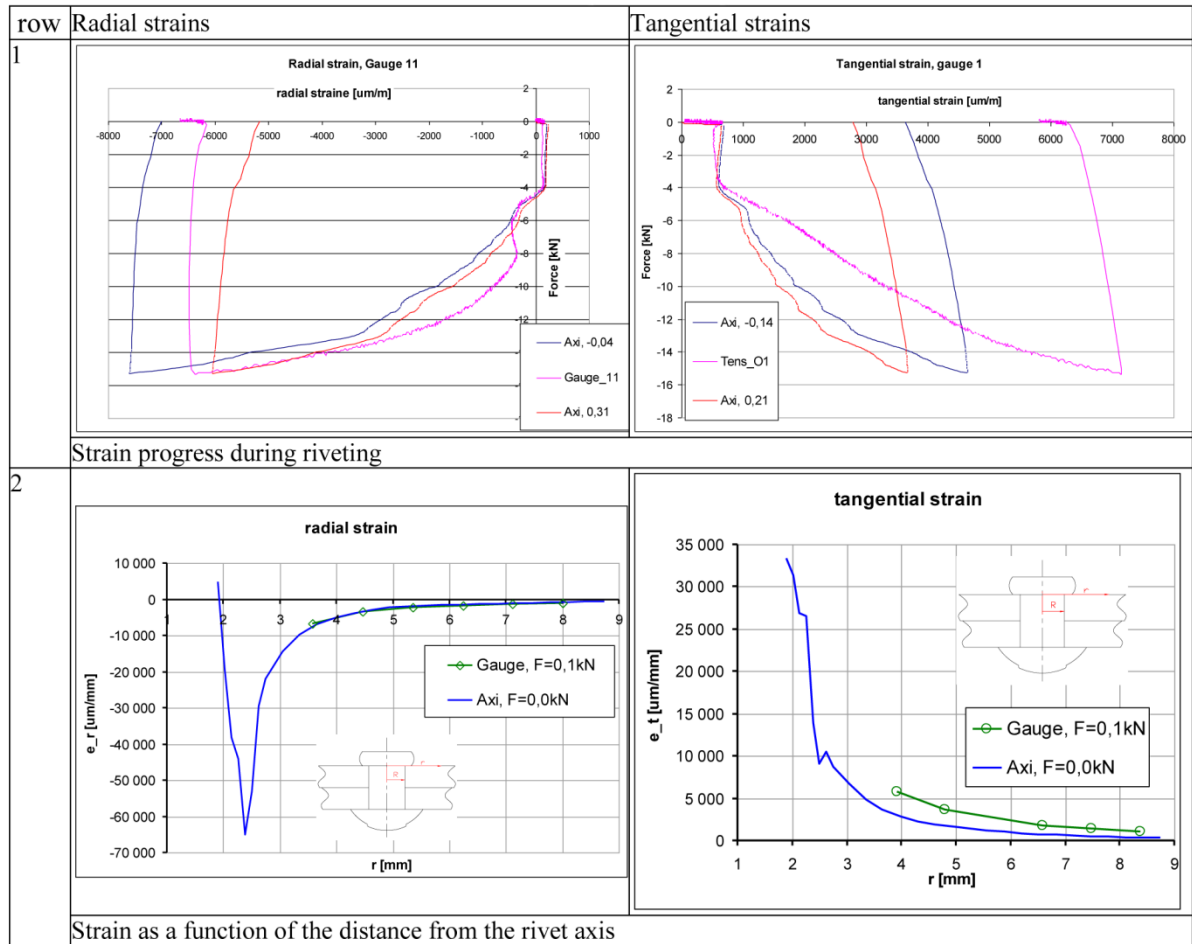
Table 4. Strains around normal brazier rivet - experiment and calculations



At the end of the riveting process numerical results agreed with the experiment but during the process differences were significant. The data for the axisymmetric and solid models did not vary much, however, in the case of tangential strains, the data from the axisymmetric model were closer to the reality. In the case of radial strains, the character of the elastic relaxation (last stage of the process) in the experiment differed from the one modeled.

Table 5 presents the results for the brazier rivet with a compensator.

Table 5. Strains around the countersunk rivet with a compensator - experiment and calculations



Very good agreement between the calculations and the experiment was obtained at the end of the riveting for radial strains. During the process, the correlation between experimental and numerical data was quite good, but the ‘S’-shaped curve was not obtained. In the case of tangential strains, the results of calculations were underestimated. The character of elastic relaxation in the experiment and in the model was similar.

CONCLUSIONS

It is commonly accepted that the residual stress system around the rivets significantly affects the fatigue life of riveted joints. Residual stresses are induced mainly during the riveting process and depend on the squeezing force value, rivet type and other factors. Müller and Hart-Smith [1] have shown that the fatigue life of investigated joints depends strongly on squeezing force while an increase in fatigue life is not linear (1.42-time increase in squeezing force resulted in a twofold increase in fatigue life; a threefold increase in force caused 11 and 25-34 time increases in fatigue life, depending on a joint configuration). The magnitude of the life increase indicates that it is not only the result of the beneficial stress system but that a change of the joint formation mechanism has taken place.

The strain progress during the riveting process was experimentally investigated for four types of rivets. Measurements confirmed very high strains near the driven head. For some types of rivets the reversal strain signal was recorded. Several numerical models were used to investigate the riveting process. Agreement between experimental and numerical results was good in some cases, while in other cases the numerical models demand/require further development. The reversal strain

effect was not obtained in calculations. This suggests that it is result of the phenomenon that has not been taken into account in numerical calculations.

It was assumed as a working hypothesis that during the riveting process the adhesive joints (called cold welding) had been formed and destroyed during the process, which was the reason why the reversal strain signal had been observed. During the preliminary investigation this hypothesis was not confirmed experimentally (the marks of the destroyed cold welding were not found). This issue will be further investigated in the future.

ACKNOWLEDGEMENT

A major proportion of the research presented here was carried out under the Eureka project E3496! IMPERJA.

REFERENCES

- [1] Müller R. P.G., Hart-Smith L.J.: *Making fuselage riveting lap splices with 200-year crack-free fatigue life*. ICAF 97. Fatigue in new and ageing aircraft. Proceedings of the 19-th Symposium of the International Committee of Aeronautical Fatigue 1997, Edinburgh, EMAS Publishing, pp.499-522,
- [2] Muller R., *An Experimental and Analytical Investigation on the Fatigue Behaviour of Fuselage Riveted Lap Joint*, TU Delft, Netherlands, 1995.
- [3] Rans C. D. *The Role of Rivet Installation on the Fatigue Performance of Riveted Lap Joints*. PhD thesis, Carleton University Ottawa, Ontario, Canada, 2007
- [4] Wronicz W., Kaniowski J., *Experimental and Numerical Study of Strain Progress During and After Riveting Process for Brazier Rivet and Rivet with Compensator – squeezing force and rivet type effect*. Fatigue of Aircraft Structures Monographic Series A. Niepokólczycki (Ed.), Institute of Aviation Scientific Publication, ISSUE 2011., pp.165-189
- [5] Szymczyk E., Jachimowicz J., Sławiński G., Derewońko A., *Influence of technological imperfections on residual stress fields in riveted joint*. Dissipation and Damage across Multiple Scales in Physical and Mechanical Systems, Oxford, United Kingdom, 2009, pp.1-4
- [6] Skorupa M, Skorupa A, Michniewicz T, Korbel A. *Effect of production variables on the fatigue behaviour of riveted lap joint*. International Journal of Fatigue 32 (2010) pp.996–1003
- [7] Langrand B., Patronelli L., Deletombe E., Markiewicz E., Drazéć P., *An alternative numerical approach for full scale characterization for riveted joint design*, Aerospace Science and Technology 6 (2002) pp. 343–354
- [8] Li, G., Shi, G., Bellinger N.C. *Studies of Residual Stress in Single-Row Countersunk Riveted Lap Joints*, *Journal of Aircraft*, Vol. 43, No. 3, 2006, pp.592-599
- [9] Wronicz W., Kaniowski J., *Analysis of the Quasi-Static Process for 90° Countersunk Rivet*, Fatigue of Aircraft Structures Monographic Series A. Niepokólczycki (Ed.), Institute of Aviation Scientific Publication, ISSUE 2012., (article in press).